Biocatalytic Carboxylation

Silvia M. Glueck,[a,b] Selcuc Gümüs,[b,§] Walter M. F. Fabian,[b] Kurt Faber[b,*]

[a] Research Centre Applied Biocatalysis, [b] Department of Chemistry, Organic and Bioorganic Chemistry, University of Graz, Heinrichstrasse 28, A-8010 Graz, Austria.

Electronic Supporting Information

Computational Results

Concerning the two computational procedures used, IEF-PCM(H_2O)-MP2/cc-pVTZ//MP2/cc-pVDZ vs IEF-PCM(H_2O)-G3MP2B3, the latter which is generally considered to provide thermochemical quantities with almost chemical accuracy (1 – 2 kcal mol^{-1})[1,2] invariably yields less positive ΔG_{react} – values than obtained by MP2. For instance, whereas the reaction in entry 24 is nearly thermoneutral with G3MP2B3, ΔG_{react} = +4.2 kcal mol^{-1} from MP2 calculations. However, the trend in reaction energies obtained by the MP2 calculations closely parallels that from the G3MP2B3 model chemistry (r^2 = 0.989). Thus, for those reaction where the IEF-PCM-G3MP2B3 calculations failed (yielding structures with small imaginary frequencies, reactions in entries 6, 8 - 10, and 14, cf. Table 1), this correlation equation might be used to estimate the corresponding IEF-PCM-G3MP2B3 reaction Gibbs free energies from the MP2 results. Furthermore, this close correspondence between the two computational approaches lends additional credence to their reliability.

All reactions except those in entries 27, 28 and possibly 24 are calculated to be endergonic (ΔG_{react} >0) thus corroborating the notion of an energetically unfavourable uphill direction of carboxylation reactions. The near thermoneutrality obtained for the carboxylation of phenylphosphate leading to 4-hydroxybenzoic acid, entry 24 in Table 1, can be attributed to the additional hydrolysis of the energy-rich phosphate ester group, compare entries 16, 23, and 24. The strong exergonic character resulting for the carboxylation of 2-methyloxirane (entry 27) clearly is due to the strain released upon opening of the three-membered ring. The carboxylation of crotonic acid (entry 28) is also a special case because the introduction of the carboxyl group goes in hand with (energetically favourable) hydrogenation to give ethyl malonate. Hence the different energetics as compared to the other carboxylation reactions. The least feasible carboxylations are obviously are those involving

§ On leave from Middle East Technical University, Ankara, Turkey.

* Corresponding author: phone +43-316-380-5332; fax: +43-316-380-9840; e-mail: <Kurt.Faber@Uni-graz.at>.

aldehyde acceptors, entries 1 – 4 with ΔG_{react} > +12 kcal mol^{-1}. Except reactions catalysed by aryl malonate decarboxylase (entires 8 and 9 in Table 1) carboxylations of acidic C-H acceptors (entries 5 – 13), and even more so, aryl C-H acceptors 16 – 22, are more favourable, ΔG_{react} ~ 7 – 10 and ~ 5 – 8 kcal mol^{-1}, respectively. Obviously, the presence of a deactivating carboxyl group in 3,4-dihydroxy benzoic acid disfavours the introduction of a second one, entry 21. Similarly, in heteroaryl C-H acceptors, entries 25 and 26, the electron-poor nature of the carboxyl-substituted pyridine ring results in one of the most endergonic reactions described here. In contrast, the electron-rich pyrrole ring is calculated as one of the most easily carboxylated substrates, topped only by the phosphorylated phenol and the strained oxirane, entries 24 and 27. Although the calculated reaction Gibbs free energies allow a crude categorisation based on the type of the CO_2-acceptor, e.g. aldehyde C-H, acidic C-H, aryl C-H, heteroaryl C-H, or strained acceptor, structural variations within one group result in some deviations from the characteristic values of ΔG_{react} of the respective group, e.g. entries 21 and 26.

Table S1 Calculated reaction Gibbs free energies (ΔG) for selected carboxylation reactions.[a]

Entry	Reaction Type	Reaction	Enzyme	ΔG [kcal/M][a]	□□□□
1	aldehyde acceptor	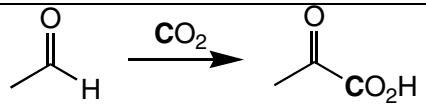	pyruvate decarboxylase	+12.4 (+14.7)	4.1.1.1
2	aldehyde acceptor	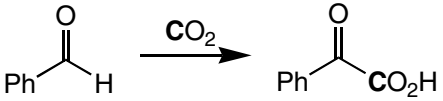	benzoylformate decarboxylase	+15.0 (+18.0)	4.1.1.7
3	aldehyde acceptor	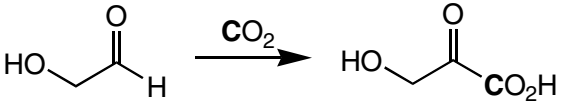	hydroxypyruvate decarboxylase	+12.7 (+15.1)	4.1.1.40
4	aldehyde acceptor	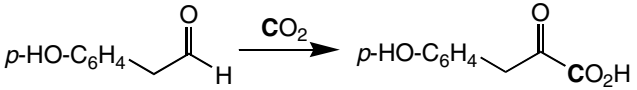	4-hydroxyphenylpyruvate decarboxylase	+13.0 (+15.4)	4.1.1.80
5	acidic C-H acceptor	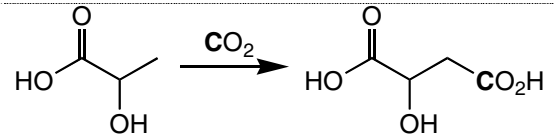	unknown	+7.2 (+11.0)	—
6	acidic C-H acceptor	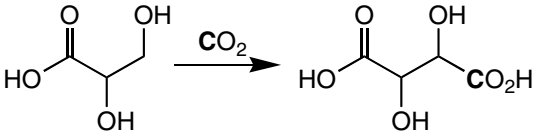	tartrate decarboxylase	+10.1[b] (+12.7)	4.1.1.73
7	acidic C-H acceptor	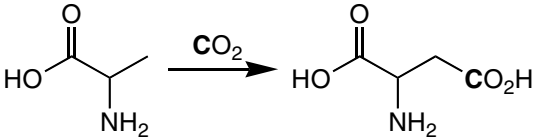	aspartate 4-decarboxylase	+7.8 (+11.1)	4.1.1.12
8	acidic C-H acceptor	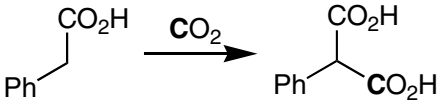	arylmalonate decarboxylase	+11.7[b] (+14.2)	4.1.1.76

9	acidic C-H acceptor	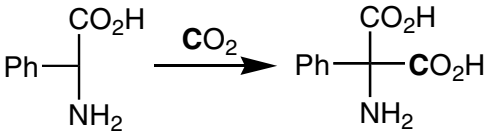	arylmalonate decarboxylase	+14.8 [b] (+17.2)	4.1.1.76
10	acidic C-H acceptor	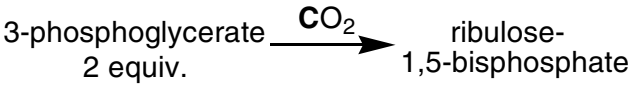	RubisCO	+7.5 [b] (+10.3)	4.1.1.39
11	C-H acidic acceptor NAD(P)H-dependent	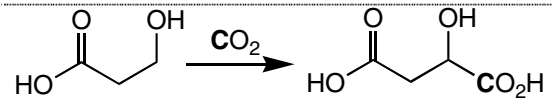	3-hydroxypropionate carboxylase	+7.7 (+11.2)	—
12	C-H acidic acceptor ATP-dependent	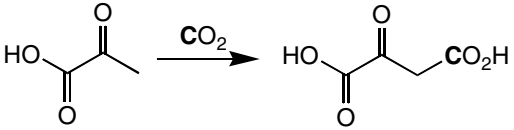	pyruvate carboxylase	+10.9 (+13.6)	6.4.1.1
13	C-H acidic acceptor ATP-dependent	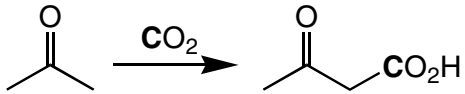	acetone carboxylase	+10.3 (+13.3)	6.4.1.6
14	amine acceptor	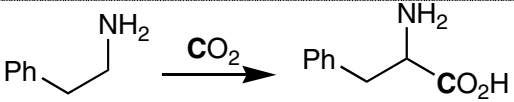	phenylalanine decarboxylase	+7.8 [b] (+10.5)	4.1.1.53
15	amine acceptor	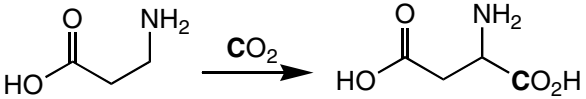	aspartate 4-decarboxylase	+7.3 (+10.1)	4.1.1.12
16	aryl C-H acceptor	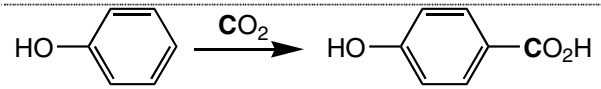	4-hydroxybenzoate decarboxylase	+6.3 (+8.8)	4.1.1.61
17	aryl C-H acceptor	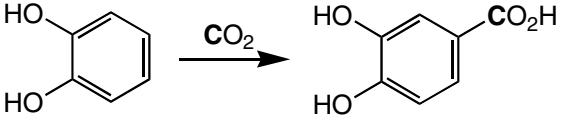	protocatechuate decarboxylase	+6.3 (+8.6)	4.1.1.63
18	aryl C-H acceptor	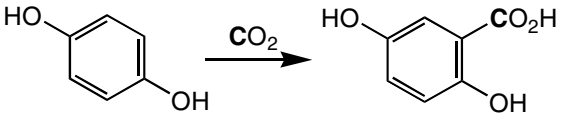	gentisate decarboxylase	+8.3 (+9.7)	4.1.1.62

19	aryl C-H acceptor	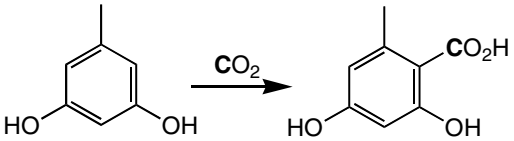	orsellinate decarboxylase	+10.3 (+11.8)	4.1.1.58
20	aryl C-H acceptor	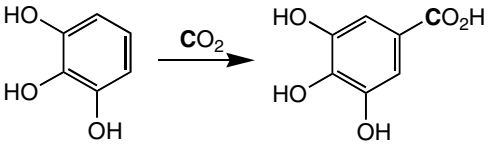	gallate decarboxylase	+6.2 (+8.5)	4.1.1.59
21	aryl C-H acceptor	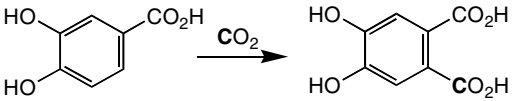	4,5-dihydroxyphthalate decarboxylase	+13.1 (+15.3)	4.1.1.55
22	aryl C-H acceptor	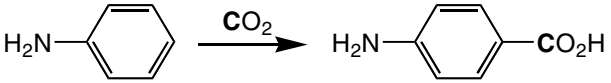	unknown	+5.3 (+8.0)	—
23	activated aryl C-H acceptor	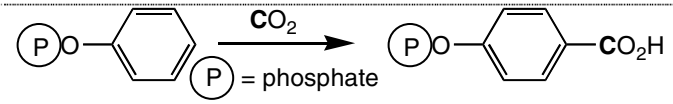	phenylphosphate carboxylase	+6.0 (+9.3)	—
24	activated aryl C-H acceptor	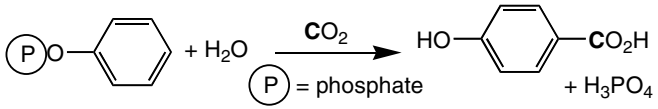	phenylphosphate carboxylase	-0.25 (+4.2)	—
25	hetero-aryl C-H acceptor	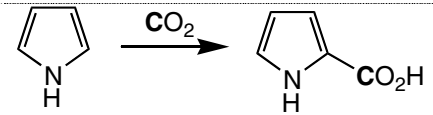	pyrrole-2-carboxylate decarboxylase	+4.8 (+6.9)	—
26	hetero-aryl C-H acceptor	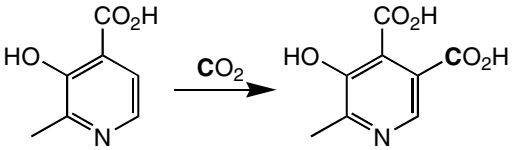	3-hydroxy-2-methylpyridine-4,5-dicarboxylate 4-decarboxylase	+14.7 (+17.6)	4.1.1.51
27	strained substrate	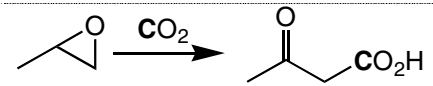	epoxide carboxylase	-18.9 (-14.6)	—
28	activated alkene	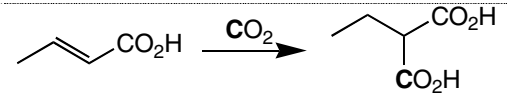	crotonyl-CoA carboxylase/reductase	-7.7 (-7.7)	—

[a] Given are Gibbs free energies from IEFPCM(H_2O)-G3MP2B3 and, in parentheses, IEFPCM(H_2O)-MP2/cc-pVTZ//MP2/cc-pVDZ calculations (1 kcal = 4.184 kJ); b estimated from the MP2-G3MP2B3 correlations.

References and Notes

1 R. Janoschek and M. J. Rossi, *Int. J. Chem. Kinet.,* 2002, **34**, 550-560; R. Janoschek and M. J. Rossi, *Int. J. Chem. Kinet.,* 2004, **36**, 661-686; W. M. F. Fabian, *Monatsh. Chem.* 2008, **139**, 309-318.

2 The geometries of all reactants and products shown in Table 1 were fully optimized by second-order Moller-Plesset perturbation theory [C. Moller and M. S. Plesset, *Phys. Rev.,* 1934, **46**, 618-622.] using Dunning's double-zeta correlation consistent basis set [T. H. Dunning, *J. Chem. Phys.,* 1989, **90**, 1007-1023] (MP2(cc-pVDZ). Solvent effects (H_2O) were estimated by MP2/cc-pVTZ single point calculations using the polarizable continuum model [J. Tomasi, B. Mennucci and E. Cances, *J. Mol. Struct. (THEOCHEM),* 1999, **464**, 211-226] (IEF-PCM-MP2/cc-pVTZ//MP2/cc-pVDZ). To assess the importance of higher-level correlation contributions to the respective reaction Gibbs free energies as well as the effect of the solvent water on optimized structures, IEF-PCM (H_2O) calculations using the G3MP2B3 model chemistry were performed according to L. A. Curtiss, P. C. Redfern, K. Raghavachari, V. Rassolov and J. A. Pople, *J. Chem. Phys.,* 1999, **110**, 4703-4709; A. G. Baboul, L. A. Curtiss, P. C. Redfern and K. Raghavachari, *J. Chem. Phys.,* 1999, **110**, 7650-7657. The Gaussian program was used for all calculations; Gaussian 03, Revision B.04; see: M. J. Frisch, G. W. Trucks, H. B. Schlegel, G. E. Scuseria, M. A. Robb, J. R. Cheeseman, J. Montgomery J. A., T. Vreven, K. N. Kudin, J. C. Burant, J. M. Millam, S. S. Iyengar, J. Tomasi, V. Barone, B. Mennucci, M. Cossi, G. Scalmani, N. Rega, G. A. Petersson, H. Nakatsuji, M. Hada, M. Ehara, K. Toyota, R. Fukuda, J. Hasegawa, M. Ishida, T. Nakajima, Y. Honda, O. Kitao, H. Nakai, M. Klene, X. Li, J. E. Knox, H. P. Hratchian, J. B. Cross, V. Bakken, C. Adamo, J. Jaramillo, R. Gomperts, R. E. Stratmann, O. Yazyev, A. J. Austin, R. Cammi, C. Pomelli, J. W. Ochterski, P. Y. Ayala, K. Morokuma, G. A. Voth, P. Salvador, J. J. Dannenberg, V. G. Zakrzewski, S. Dapprich, A. D. Daniels, M. C. Strain, O. Farkas, D. K. Malick, A. D. Rabuck, K. Raghavachari, J. B. Foresman, J. V. Ortiz, Q. Cui, A. G. Baboul, S. Clifford, J. Cioslowski, B. B. Stefanov, G. Liu, A. Liashenko, P. Piskorz, I. Komaromi, R. L. Martin, D. J. Fox, T. Keith, M. A. Al-Laham, C. Y. Peng, A. Nanayakkara, M. Challacombe, P. M. W. Gill, B. Johnson, W. Chen, M. W. Wong, C. Gonzalez and J. A. Pople, Gaussian, Inc., Wallingford CT, 2004.